American Journal of Polymer Science and Technology
2023; 9(4): 45-54
http://www.sciencepublishinggroup.com/j/ajpst
doi: 10.11648/j.ajpst.20230904.11
ISSN: 2575-5978 (Print); ISSN: 2575-5986 (Online)

Study on the Morphological and Mechanical Properties of Polyvinyl Chloride Reinforced with Snail Shells

Levi Dooga[1, *], Casimir Emmanuel Gimba[2], Hamza Abba[2], Abdulrahman Musa[2]

[1]Department of Chemistry, Benue State University, Makurdi, Nigeria

[2]Department of Chemistry, Ahmadu Bello University, Zaria, Nigeria

Email address:

doogalevi@gmail.com (Levi Dooga)

[*]Corresponding author

To cite this article:

Levi Dooga, Casimir Emmanuel Gimba, Hamza Abba, Abdulrahman Musa. Study on the Morphological and Mechanical Properties of Polyvinyl Chloride Reinforced with Snail Shells. *American Journal of Polymer Science and Technology.* Vol. 9, No. 4, 2023, pp. 45-54. doi: 10.11648/j.ajpst.20230904.11

Received: August 27, 2023; **Accepted**: September 12, 2023; **Published**: October 8, 2023

Abstract: In this work, the authors melt blending method fabrication of the composites. The physico-chemical, morphological and mechanical properties of the composites were investigated. The test results showed that, there was an improvement at all level. The optimal impact strength and tensile strength of the studied composite were 3441.79 MPa and 6.021 MPa. The flexural strengt was noted to improve from 11.92 MPa to 16.79 MPa. The incorporation of Snail shells to PVC blends decreased the density from 1.34 gcm^{-1} to 1.18 gcm^{-1} while water intake was noted to decrease from 0.18% to 0.12%. The FTIR revealed OH, which is an indication of the material hydrophobic nature. The stretching vibration of aliphatic C-H in the PVC structure was at 2918.5 and 2855.1 cm^{-1} in the control PVC blends corresponds with. The C=C bond of aromatic functional group at; 1602.8 cm^{-1} in the composites. The FTIR examination of the control PVC had absorption band at 1423.8 cm^{-1} corresponding to $–CH_2$ of methylene group. The absorption band 1453.7 cm^{-1} corresponds with $–CH_2$. It can also be observed that, the control PVC blend showed no absorption band that corresponds with $–CH_3$. This is due to absence of a methyl group in the structure of polyvinyl chloride. The absorption band noticed in all the samples is that of absorption peaks of 697.0 and 752.9 cm^{-1} which corresponds to C-Cl bond which represents a chloride functional group in PVC. The SEM analysis showed that, the Snail Shell were uniformly dispersed in the polymer blends and, explained the improved mechanical properties observed in the study.

Keywords: Polyvinyl Chloride, Polystyrene, Polypropylene, Snail Shells, Mechanical Properties

1. Introduction

The need to enhance the properties of polymer has become necessary in order to produce materials that can withstand drawbacks that cause catastrophic failure of properties during applications [1]. Research has shown that the use of polymer-based composites result in novel material formulations. Moreover the manufacture of profiles with optimal properties for special applications is also made possible. Polymer composites lead to improvement in product design and reduction in energy usage [2]. However, the cost and processing difficulties involved in the use of mineral-based filler leads to a search for an alternative fillers. Mineral limestone or calcium carbonate have widely be used in the reinforcement of polymer as inorganic filler. Snail shells as a bio-material contains high content of calcium carbonate and can replaced mined limestone. They are abundant and are discarded by-products which can serve as potential substitutes for limestone derived from sedimentary rocks [3]. Agricultural waste derived from plants and animals such as nut shells, fibers and bones have gained attention of researchers. These substances are the major part of the waste produce in the urban and rural area. They attract the attention of insect such as mosquitos, snake and lizard to the environment as well as the gaseous

pollutants they release into the air when burnt [4].

2. Materials and Methods

2.1. Sample Preparation

Waste materials made of Polyvinyl Chloride, Polypropylene and Polystyrene polymers were sourced within Ahmadu Bello University, Zaria building sites. The materials were washed thoroughly with distilled water and crushed using shredding machine. The Snail shells were collected locally at Ahmadu Bello University farmer in a clear polyethene bag and transported to the Prof. J. Y. Olayemi Laboratory, Department of chemistry, Ahmadu Bello University, Zaria. The snail were removed from its shells and washed with clean water to remove any adhered hard particles. The shells were dried at room temperature 30 days until a constant weight was observed, after which the shells samples were grinded into powder with the use of ball miller machine. The grinded powder was sieved with BS/ISO 3310 into 150 μm and 75 μm particle sizes. The sieved sample was stored separately in a plastic containers and labelled for further research work [2].

2.2. Composites Development

The samples of Polyvinyl Chloride, Polypropylene, Polystyrene and filler samples were weighed using the electronic balance. The two roll-mill was set at a processing temperature of 190°C. The nip of the rollers was adjusted and polymer matrixes were poured for blends formation. Incorporation of fillers was done immediately after the total melting of the polymers and the composites was formed. Then, the composites were naturally cooled for 6 minutes in compression molding machine under 15 MPa at room temperature. The molded composites sheets were cut to appropriate sizes for further analysis [2, 5].

2.3. Mechanical Property Testing

Impact, Hardness, Tensile and Flexural test were carried out on the composites to determine the mechanical behavior of the composites. Impact strength test was carried out in accordance with ASTM using charpy impact machine of model number 412 of capacity 15J for polymer composites at room temperature. A test piece of dimension 100mm×4mm was cut and placed in the impactor sample holder, and the impact hammer was released and the impact values was recorded as averages [6]. The hardness test was conducted according to ASTM D2240-08-2018 method. The sample was placed on the hard flat surface of the machine and the machine indentor pin was force to penetrate the sample. The readings were manually recorded as the pointer of the hardness tester stop at a given calibration of the machine [7]. The tensile strength test was carried out using Tensometer 9875 type W, in accordance with the ASTM D638 method. The composite sample was cut into dumbbell shape and inserted into the tensometer. The sample was stretched in the testing machine at a uniform rate of 26mm/min, and the force (KN) on the specimen and corresponding extension was simultaneously measured until the specimen broke [4, 8]. The flexural test was conducted according to ASTM D7264-2018. The specimen was placed on the machine-supported beam and then, the force was applied at the centre of the specimen sample and the values of the strength were recorded as the sample reached its maximum bend [9].

2.4. Water Adsorption

Water adsorption test was carried out according to ASTM D570 [7]. The specimens were and weigh and immerse in distilled water for 48 hours, after which the specimens were removed weigh again. Both weight before and after immersing in water were recorded and the data obtained were used to determine percentage water adsorption using the formula below;

$$\%\ water\ intake\ = \frac{\text{Weight After} - \text{Weight before}}{\text{Weight before}} \times 100 \qquad (1)$$

2.5. Density Test

The density of the specimens were determined according to Archimede's Principle based on the assumption that water used for immersion has a density of 1 gcm^{-3} using the equation below [10];

$$Density = \frac{\text{Mass of sample}}{\text{volume of the sample}} \qquad (2)$$

2.6. Morphology Test

Samples were coated with platinum coating of electrically conducting material, deposited on the sample either by low-vacuum sputter coating or by high-vacuum evaporation. The morphology of the cross-section of the polymer composites was examined by scanning electron microscopy (SEM), at a magnification of 9000x by means of a PhenomProX scanning electron microscope (SEM) with an energy dispersive spectroscope (EDS), operated at 15kV [11].

2.7. X-ray Diffraction Test

The X-ray diffraction analysis was conducted using Rigaku D/Max.IIIc PW 1800 X-ray Diffractometer. The samples were loaded onto the machine in the sample chamber of the rigaku X-ray diffraction machine. The optimum voltage (55 kv) and an optimum current (35 mA) were applied to produce the X-rays to excite the sample for pre-set time (10 minutes) in the case. The spectrum obtained from the samples was analysed to ascertain the constituent interfacial interaction and possible increase in the crystalline property of the samples [12].

2.8. Fourier Transform Infrared

FTIR analysis on the composites were carried out using KBr disc in the range oof 4000 to 400 cm^{-1} in the multi-user Laboratory, Ahmadu Bello University, Zaria to determine the

functional groups present in the composites.

3. Results and Discussion

3.1. Mechanical Properties

3.1.1. Impact Strength

It showed in Figure 1 that, the impact strength of the control blends was 2638.70 MPa. However, at the addition of PP and PS to the blend without filler, the impact was noted to increase to 2868.16 MPa and 3785.97 MPa. This is an evidenced of phase transition to hardness of the material. In a related research, the impact strength a polymer blends increased as the composition changed [13]. The material continue in a similar impact strength increment as 3097.61 MPa obtained with the addition of 150 µm particle sizes and 3441.79 75 µm particle sizes. In related studies, increased impact strength is reported with increase filler content of composites [14]. According to reports, the improved results observed is due to proper interfacial bonding between the blends and the fillers. However, the impact strength of some of the composites were noted to decrease to 2523.98 MPa as result of poor dispersion of filler into the blends matrices and expede crack propagation [14].

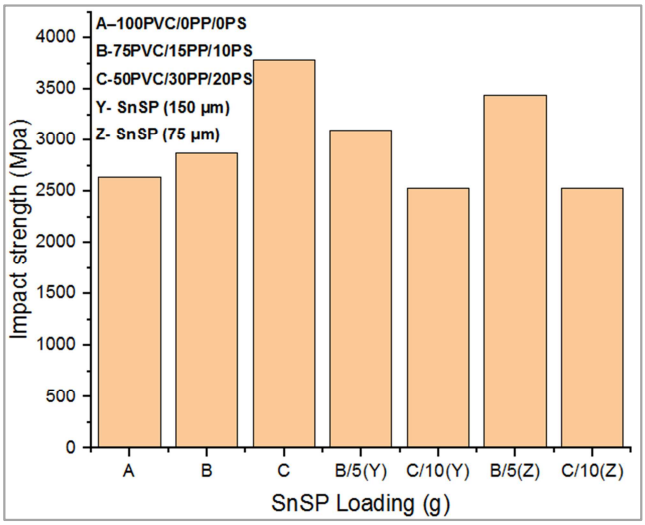

Figure 1. *Effect of Snail Shells Filler Loading on the impact strength of the Composite.*

3.1.2. Hardness Strength

The control PVC blend shows optimum hardness strength of 98.33% as depicts in Figure 2. However, the cross linking behavior of the constituents matrices were affected as PP and PS were added to the blends without filler due to the brittle nature of PP [15]. The addition of 150 µm filler particle sizes revealed 97.00% and 96.96% whereas, 98.00% and 95.67% were noted with the addition of 75 µm filler particle sizes. Optimum hardness strength of 98.00% was obtained with tiny filler particle sizes. Similar study reported highest hardness strength at 63 µm filler particle size and, attributed the observation to the ease to which smaller particles are distributed within the blends and form better adhesion as a result of good interfacial interaction [4].

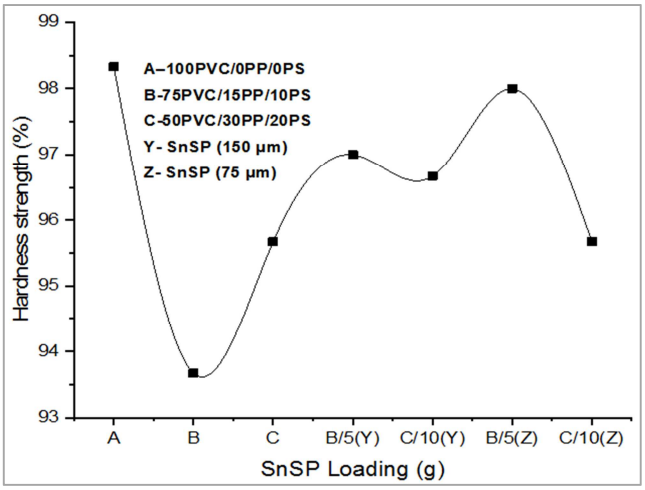

Figure 2. *Effect of Snail Shells Filler Loading on the Hardness strength of the Composite.*

3.1.3. Tensile Strength

The effect of fillers loading on the tensile strength of the material was studied. The tensile strength of the control blend without filler was 4.331 MPa as shown in Figure 3. However, as PP and PS were added to the PVC, the tensile strength increase to 4.573 MPa, and 7.08 MPa. Related studies reported increased trend of the tensile strength under various compositions of PS in PP [16]. The incorporation of 150 µm sizes of Snail shells to the blends increases the tensile strength of the composites to 6.021 MPa and 6.655 MPa. This is comparably higher than the 4.331 MPa of the control PVC blend. The implication is that, there is a better interaction between the blend and filler for strong bond formation [13]. The addition of 75 µm particle sizes of the filler revealed 6.161 MPa and 3.499 MPa. The poor value of 3.499 MPa obtained is due to agglomeration of Snail shells particles in the composites and, this is detrimental the mechanical properties of the composites [17].

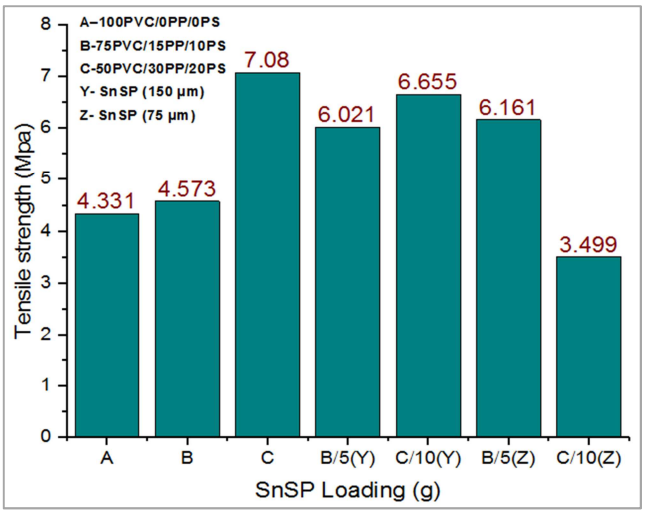

Figure 3. *Effect of Snail Shells on the Tensile strength of the Composite.*

3.1.4. Percentage Elongation

The effect of blend composition and Snail shells filler loading on percentage elongation is displayed in Figure 4. The control blend of PVC had a percentage elongation of 2.107 %. However, as the PP and PS in the blend increased, the percentage elongation also increased to 2.528% and 3.652%. Study on alpha olefin and ethylene propylene diene rubber also reported similar gradual increase in percentage elongation as ethylene octane copolymer (EOC) content increases in the blend. The addition of 150 µm particles of Snail shells increased the percentage elongation to 4.093% after which, it gradually decreases to a value of 3.055% as well as 3.199% and 2.949% with the addition of 75 µm filler particle sizes. The decrease trend conforms to a related study that reports gradual decrease in percentage elongation with the addition of filler material [18]. The decrease observed is because, the addition of the filler to blend increase the intermolecular van der waals forces between the polymers which increase stiffness and reduces flexibility of the composites [19].

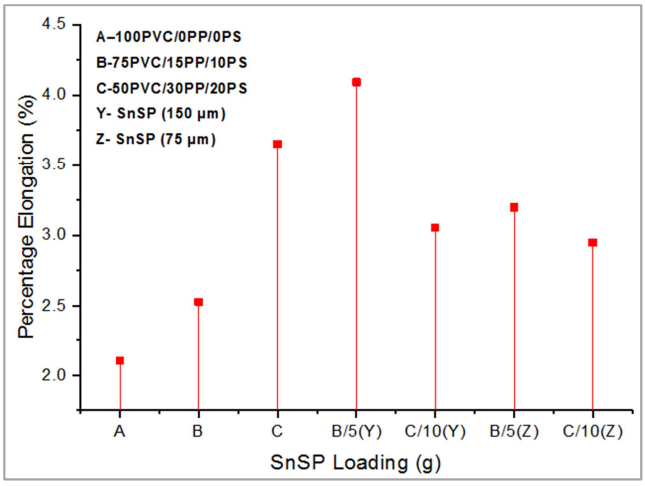

Figure 4. *Effect of Snail Shells filler on the percentage elongation of the Composite.*

3.1.5. Tensile Modulus

From the result presented in Figure 5, the blend of control PVC recorded a tensile modulus of 205.55 MPa and decrease to 180.89 MPa and 193.87 MPa the amount of PP and PS in the blend increased without filler incorporation. The decrease is observed even with the addition of Snail shells into the blend to examine the effect of filler loading on the tensile modulus of the composite material. The results obtained with 150 µm filler particle sizes are 147.11 MPa and 217.84 MPa whereas, 192.59 MPa and 118.65 MPa were obtained with 75 µm filler particle sizes. The high value of 217.84 MPa recorded agreed with other studies that also reported improved tensile modulus [20]. Since tensile modulus is a function of both strength and elongation within elastic limit. It means that, the filler loading produced high strength and low elongations which resulted to the 217.84 MPa tensile modulus observed [4].

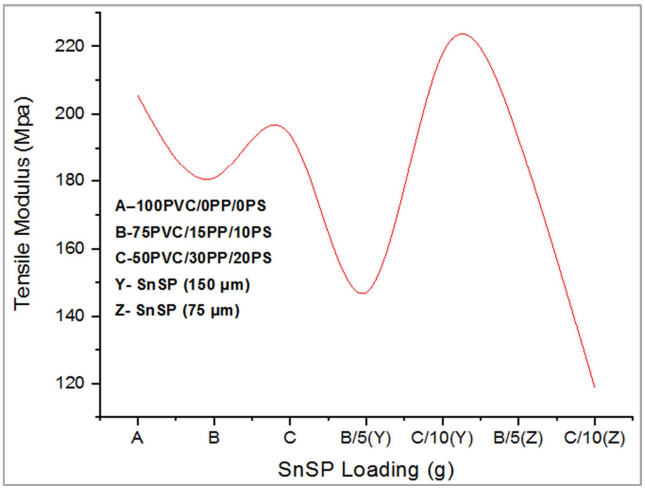

Figure 5. *Effect of Snail Shells filler on the Tensile Modulus of the Composite.*

3.1.6. Flexural Strength

The addition of PP and PS to PVC increase the flexural strength of 11.92 MPa observed in the PVC control blend to 14.49 MPa as shown in Figure 6. However, the addition of 150 µm filler particle sizes revealed 12.34 MPa and 9.06 MPa respectively. The results follows an irregular pattern, however agreed with the report of [21], who noted initial increase in the flexural strength of a bio-nanocomposites. The study reported that, as the amount of nano-crystalline cellulose in the composite increase, the flexural strength gradually decreases. The addition of tiny particles of 75 µm filler particle sizes showed 6.73 MPa as well as a high value of 16.79 MPa. Smaller filler particle sizes offered better dispersion and improved interaction between filler and the blend at various filler loading is responsible for the trend observed in the flexural strength of the study [4].

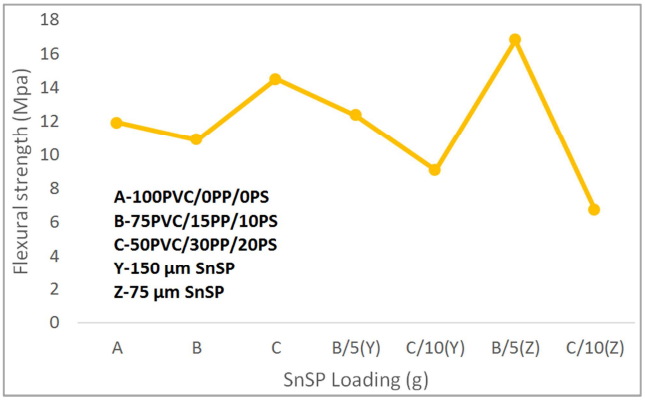

Figure 6. *Effect of Snail Shells filler on the flexural strength of the Composite.*

3.1.7. Flexural Modulus

In Figure 7, the results of the effect of filler loading on the flexural modulus of the control PVC blend was 1648.480 MPa and decreased to 749.120 MPa as PP and PS are added to the blend without filler incorporation. The results agreed with the high flexural modulus of 3224 MPa and 2588 MPa reported by a similar study [22]. The evaluation of the effect

of snail shells using 150 µm particle sizes revealed 2027.958 MPa and 839.354 MPa whereas, the use of 150 µm particle sizes revealed 2125.430 MPa and 900.217 MPa respectively. The low flexural modulus of 839.454MPa and 900.217 MPa was observed at high filler contents and can be attributed to low flexural force and high deflection of the material within elastic limit [4].

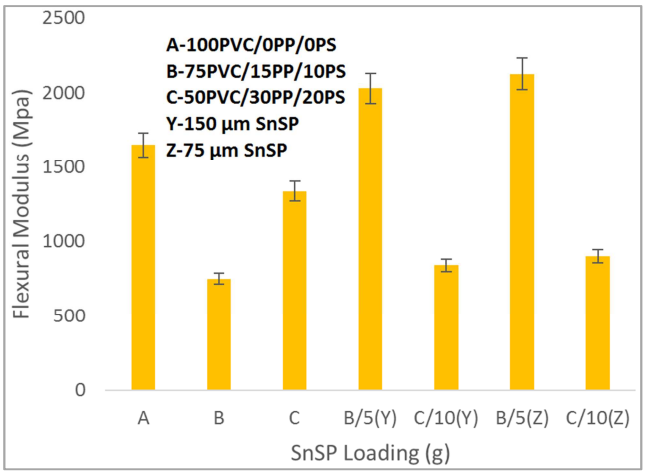

Figure 7. *Effect of Snail Shells filler on the flexural modulus of the Composite.*

3.2. Characterisation

3.2.1. Scanning Electron Microscope

The surface morphology analysis of the composites were carried out using Scanning Electron Microscopy (SEM) at 9000x magnification as shown in Figure 8, it can be seen in (a) that, the micrograph of the control PVC blend shown an irregular configuration of its molecules. The particles agglomerated and voids formation was observed on the surface of the materials. The presence of the voids is a sign of weak interfacial interaction of the PVC molecules and explained why the blend showed poor tensile and flexural strength when compared with the composites [23]. The morphology of Snail shells at 150 µm filler particle-sized shown in (b) revealed the presence of agglomerations and voids on the surface of the material. The voids are caused by large diameter of the filler and may prevent the entry of hardener into filler and act as stress concentrations, leading to low adhesion and poor compatibility between filler and blends and so, affecting the mechanical performance [24]. In (c), it can observed clearly that, there was a proper distribution of filler particles across the blends. This leads to good interfacial interaction between the filler and the blends and, explained why the mechanical properties of the composites improved [2].

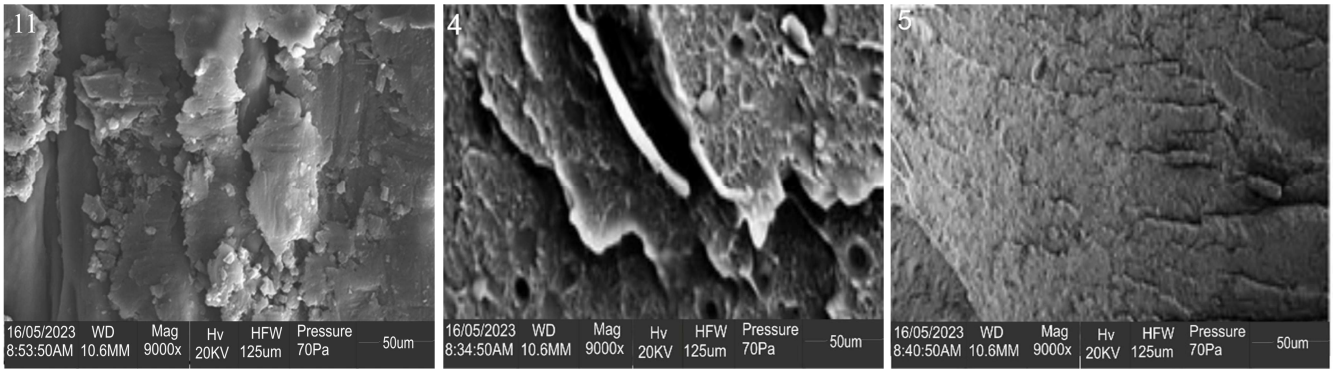

(a) (b) (c)

Figure 8. *SEM micrograph of (a) 75PVC/15PP/10PS/5SnSP blends (b) 75PVC/15PP/10PS/5SnSP Composites (150 µm) (c) 75PVC/15PP/10PS/5SnSP Composites (75 µm).*

3.2.2. The Fourier Transform Infra-Red (FTIR)

FTIR is used as an approach to study the water absorption behaviour of a polymer based on the functional group of the material as shown in Figure 9. It can be observed in (a), (b) and (c) that, the control PVC blend presents weak spectra band between the range of 3384.4 and 3749.7 cm^{-1} which corresponds to the hydrogen bond OH stretching and, suggests the weak hydrophilic nature of the control PVC blend [25]. The OH group disappeared as fillers of different particle size were introduced. This is an indication that, the hydroxyl groups had reacted completed [26]. Also, the characteristic absorption bands at 2918.5 and 2855.1 cm^{-1} in the control PVC blends corresponds with the stretching vibration of aliphatic C-H in the PVC structure [27]. The C-H bond becomes more pronounced as more hydrogen and carbon atom are introduced due to PP, PS and fillers addition to the blends. The addition of PS to the control PVC introduced C=C bond of aromatic functional group at 1602.8 cm^{-1} in composites. The indication of the presence of C=C stretching is in line with the study of [28] who reported that, the existence of one or more aromatic rings in a structure is normally readily determined from the CH and C=C-C ring-related vibrations. Another peak observed in the control PVC is at 1423.8 cm^{-1} corresponding to $–CH_2$ of methylene group. Both the blends with and without fillers exhibits stretched at 875.9 and 685.8 cm^{-1} corresponding to C-Cl bond [29].

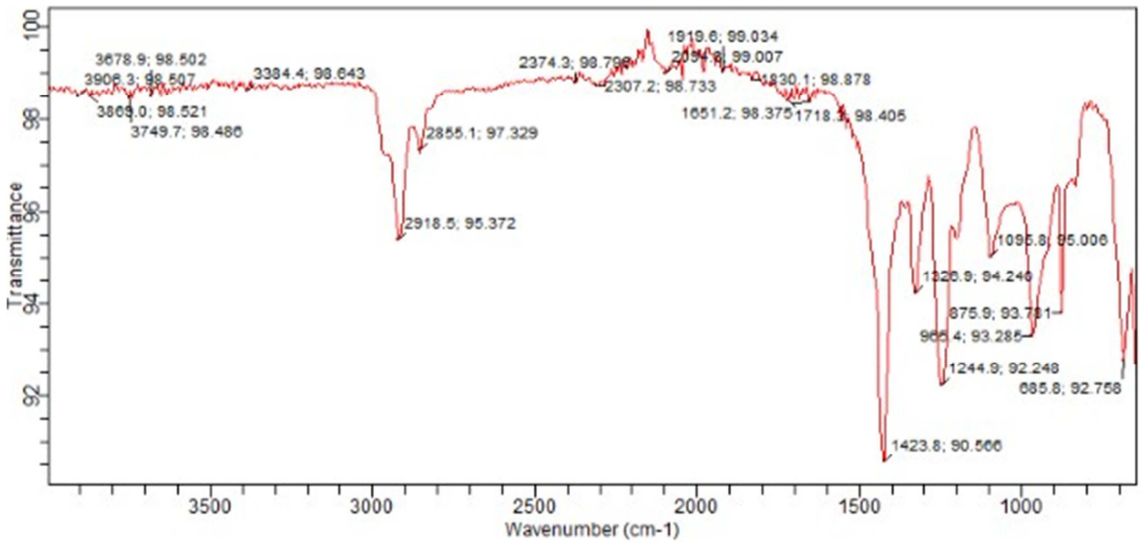

(a)

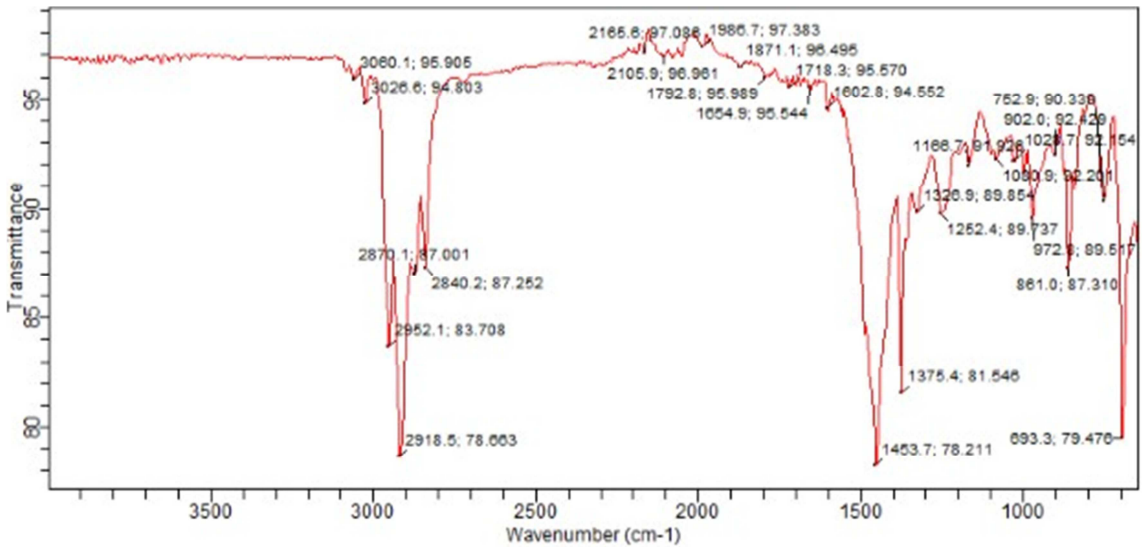

(b)

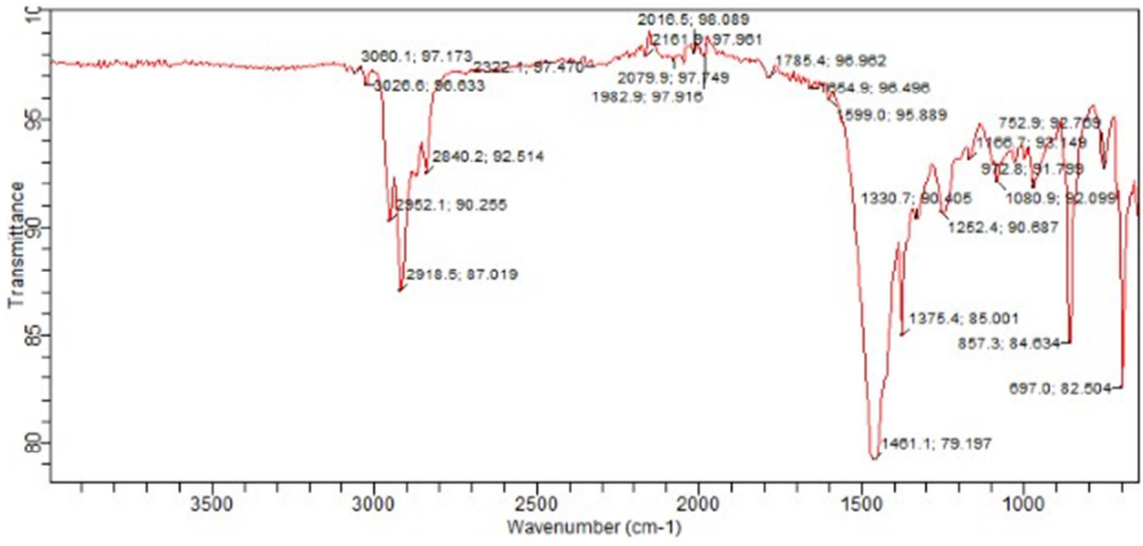

(c)

Figure 9. *FTIR of (a) 100PVC/0PP/0PS blends (b) 75PVC/15PP/10PS/5SnSP Composites (150 µm) (c) 75PVC/15PP/10PS/5SnSP Composites (75 µm).*

3.2.3. X-Ray Diffraction

The XRD analysis was carried out to determine the crystalline characteristics of the composites as shown in Figures 10. It can observed in (a), (b) and (c) of Figures 10 that, result of 100PVC/0PP/0PS blends have two prominent peaks with reflection angles at 2Θ = 14.93° and 17.69°. The diffractogram of 50PVC/30PP/20PS/10SnSP composites with 75 µm particle size indicated main characteristic peaks at 2Θ as 14.91°, 17.72° and 19.35°. However, the four prominent peaks (14.99°, 17.74°, 19.55° and 22.44°) were noticed at 2Θ as reflection angles in 75PVC/15PP/10PS/5SnSP composites with 150 µm particle size. The values of 2Θ increased with increase in the relative intensity of the composites. The intensity of spot on diffraction is directly proportional to the electron density as well as the possible of finding molecules which is also proportional to its structural crystallinity of the molecules [30]. The control PVC blend blends without fillers showed 63.34% crystalline nature. The incorporation of 75 µm particle size of fillers in 50PVC/30PP/20PS/10SnSP and 150 µm particle size in 75PVC/15PP/10PS/5SnSP showed 57.67% and 55.91%. The composite with optimal percentage crystallinity had 57.67%. The optimal percentage crystallinity of composites obtained is due to increased chain rearrangement of pendant groups such as methyl and benzene group in polypropylene and polystyrene present in the composites constituents. [31].

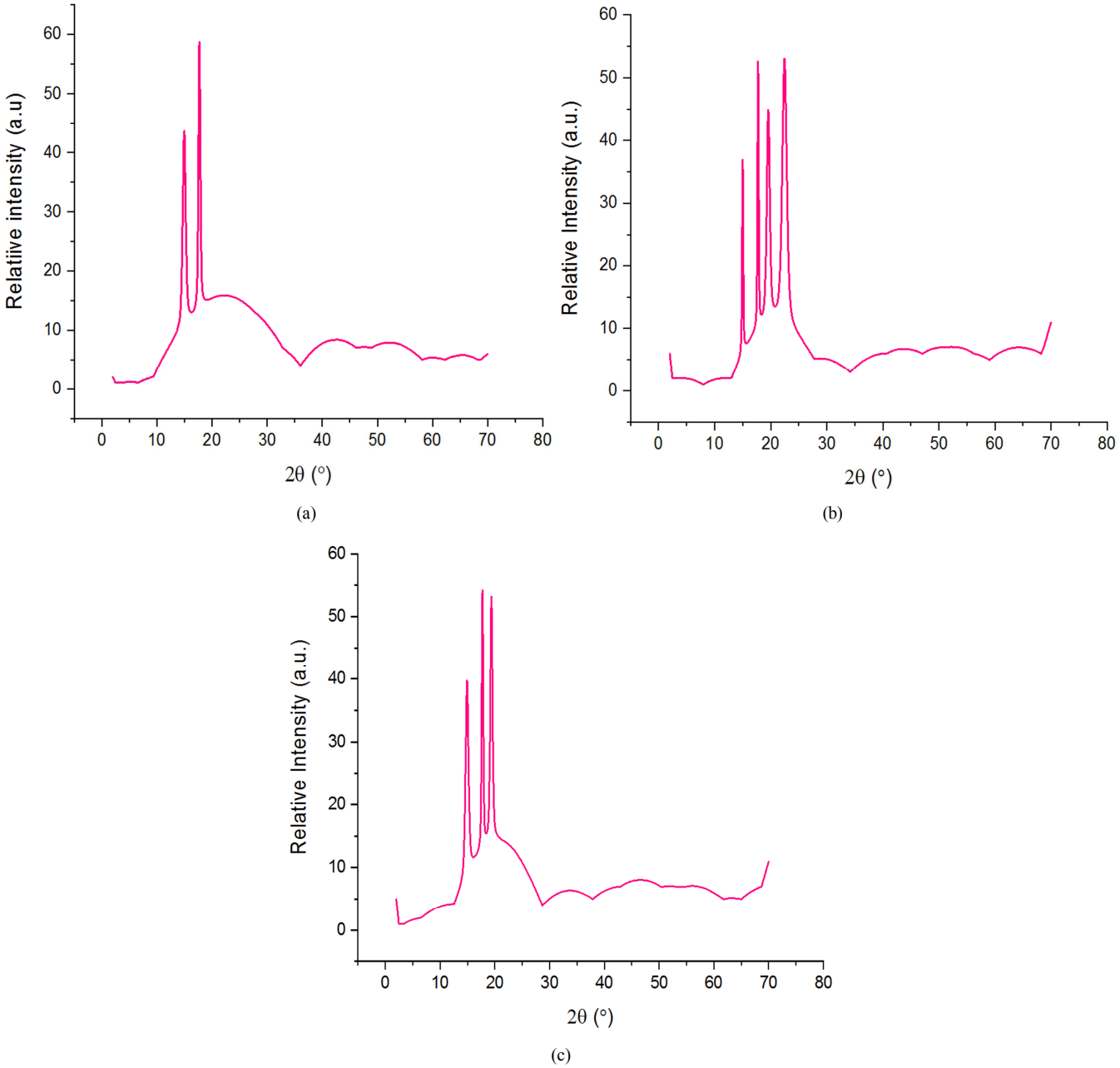

Figure 10. *X-ray of (a) 100PVC/0PP/0PS blends (b) 75PVC/15PP/10PS/5SnSP Composites (c) 50PVC/30PP/20PS/10SnSP Composites.*

3.3. Physico-Chemical Analysis

Limited densities of polymers is among the reasons they gained preference selection over conventional materials in industrial applications nowadays. For a composite polymer, the density depends on the nature and relative percentage of the polymer matrix and the filler material [32]. In Table 1, the blend of control PVC is noted to have highest density of 1.34 gcm^{-1} when compared with the blends with PP, PS and fillers. However, the density of the blends decreased to 1.29 gcm^{-1} and 1.12 gcm^{-1} as the content of PP and PS increased in the blends without filler incorporation. The decrease in the density is due to the increasing amount of PP and PS known to have lower densities in the blends. From a related study, the density of PVC is reported to be 1.30 to 1.50 gcm^{-1}, PP have 0.89 to 0.91 gcm^{-1} while PS have 1.04 to 1.08 gcm^{-1} [33]. It was also observed that, the density decreased as 75 µm Snail shells particle sizes were added. The results obtained with 150 µm Snail shells particle-sized are: 1.23 gcm^{-1} and 1.20 gcm^{-1}. These observations are in agreement with the findings of a similar research that attributed the decreased in the density of composite to better interfacial interaction between the matrix and the filler and, further explained why the composites showed improved mechanical properties [34]. Water absorption test was carried out and the results are presented in Table 1. The essence of the analysis was to check the level of moisture in the composites that would affect the functionality of the material under application. The percentage water absorption of the control PVC blend is 0.18%. The addition of PP and PS to the blends without fillers showed 0.20% and 0.16% respectively. The optimum percentage absorption of 0.20% observed for blends without filler can be attributed to proper interfacial bonds between the matrices that led to gaps for easy water intake [35]. The water adsorption of blend filled with Snail shells particle sizes of 150 µm were 0.12% and 1.99%. The incorporation of 75 µm particle size of Snail shells to the same blends compositions showed percentage water intake of 0.17% and 0.18% respectively. Since the presence of voids is an important factor in the water absorption of a polymer material, the low water intake observed is attributed to proper filler distribution across the blends as can be seen in Figure 8 of the study. However, high water adsorption of 1.99% was also observed. Other studies have reported that, poor wettability and interfacial adhesion between fillers and polymer matrix can cause hydrophilicity of the composite [14].

Table 1. *Effect of Snail shells loading on the Density and Water adsorption of PVC/PP/PS blends and PVC/PP/PS/SnSP composites.*

S/NO	Sample	Density (gcm^{-1})	Water Adsorption (%)
1	100PVC/0PP/0PS	1.34	0.18
2	75PVC/15PP/10PS	1.29	0.20
3	50PVC/15PP/10PS	1.12	0.16
4	75PVC/15PP/10PS/SnSP (150 µm)	1.23	0.12
5	50PVC/15PP/10PS/SnSP (150 µm)	1.20	1.99
6	75PVC/15PP/10PS/SnSP (75 µm)	1.19	0.17
7	50PVC/15PP/10PS/SnSP (75 µm)	1.18	0.18

4. Conclusion

From the analysis on the effect of Snail shells particles on the mechanical properties of polyvinyl chloride carried out, it was found out that, the interaction between a polymer blend and the snail shell is a physical interact and do not involve a chemical reaction. Mechanical properties such as impact strength was improved from 2638.70 MPa to 3441.79. Tensile strength was improved from 4.331 MPa to 6.655 MPa. Percentage elongation was improved from 2.107 % to 4.093 %, Young modulus was improved from 205.55 MPa to 217.84 MPa, Flexural strength and modulus were improved from 11.92 MPa and 1648.480 MPa to 16.79 MPa and 2125.430 MPa. The presence of voids in a polymer-filler bond is also caused by large diameter of the filler and may prevent the entry of hardener into filler and act as stress concentrations, leading to low adhesion and poor compatibility between filler and blends. The presence of cracks, voids and agglomeration can cause poor mechanical and sorption behaviour of the composites.

Conflicts of Interest

The authors declare there are no conflicts of interest.

References

[1] Abdel-Gawad, N. M. K., El Dein, A. Z., Mansour, D. -E. A., Ahmed, H. M., Darwish, M. M. F. and Lehtonen, M. (2017). Enhancement of dielectric and mechanical properties of Polyvinyl Chloride nanocomposites using functionalized TiO2 nanoparticles," in IEEE Transactions on Dielectrics and Electrical Insulation, vol. 24, no. 6, pp. 3490-3499, Dec. 2017, doi: 10.1109/TDEI.2017.006692.

[2] Adeosun, S. O., Akpan, E. I. and Akanegbu, H. A. (2015). Thermo-mechanical properties of unsaturated polyester reinforced with coconut and Snail shells. *International journal of composite material,* 5 (3): 52-64.

[3] Owuamanam, S., & Cree, D. (2020). Progress of Bio-Calcium Carbonate Waste Eggshell and Seashell Fillers in Polymer Composites: *A Review. Journal of Composites Science, 4 (2), 70.* doi: 10.3390/jcs4020070.

[4] Mark, U. C., Madufor, I. C., Obasi, H. C., & Mark, U. (2019). Influence of filler loading on the mechanical and morphological properties of carbonized coconut shell particles reinforced polypropylene composites. *Journal of Composite Materials, 002199831985607.* doi: 10.1177/0021998319856070.

[5] Chen, R., Liu, X., Han, L., Zhang, Z. and Li, Y. (2020). Morphology, thermal behavior, rheological, and mechanical properties of polypropylene/polystyrene blends based on elongation flow. 1–11. https://doi. org/10.1002/pat.4998

[6] Abioye, T. E., Zuhailawati, H., Anasyida, A. S., Yahaya, S. A., and Dhindaw, B. K. (2019). Investigation of the microstructure, mechanical and wear properties of AA6o61-T6 friction stir weldment with different particulate reinforcement addition. *Journal of materials Research and Technology,* 8 (5): 3917-3928.

[7] Tinastepe, N., Malkondu, O., and Kazazoglu, E. (2023). Hardness and surface roughness of differently processed denture base acrylic resins after immersion in simulated gastric acid. *The journal of prosthetic Dentistry.*

[8] Punyapriya, M. (2012). Statistical Analysis for the Abrasive Wear Behaviour of Bagasse Fibre Reinforced Polymer Composite. *International Journal of applied Research in Mechanical Engineering (Ijarme),* 2 (2): 562-567.

[9] Jacob, J., Mamza, P., Ahmed, A., and Yaro, S. (2018). Effect of benzoyl chloride treatment on the mechanical and viscoelastic properties of plantain peel powder-reinforced polyethylene composites. *Science world journal,* 13 (4): 25-29.

[10] Sommerhuber, P. F., Wang, T. and Krause, A. (2016). Wood-plastic composites as potential applications of recycled plastics of electronic waste and recycled particleboard. *Journal of Cleaner Production*.

[11] Aigbodion, V. S., Hassan, S. B., Ause, T. and Nyior, G. B. (2010). Potential Utilization of Solid Waste (Bagasse) Ash). *Journal of Minerals and Mineral Characterization Engineering,* 9, 67-77.

[12] Elmanovich, I. V., Stakhanov, A. I., Zefirov, A. A., Pavlov, A. A., Lokshin, B V. and Gallyamov, M. O. (2020). Thermal oxidation of polypropylene catalysed by manganese oxide aerogel in oxygen-enriched supercritical carbon dioxide. *The journal of supercritical fluids,* 158, 104744.

[13] Tan, W., Muyiyadi, M. and Ooi, Z. (2019). Characterization and feasibility of mimusops elengi seed shells powder as filler for thermoplastic material. *AIP conference proceedings,* 2157, 1-8.

[14] Oladele, I. O., Adediran, A. A., Akinwekomi, A. D., Adegun, M. H., Olumakinde, O. O., & Daramola, O. O. (2020). Development of Ecofriendly Snail Shells Particulate-Reinforced Recycled Waste Plastic Composites for Automobile Application. *The Scientific World Journal,* 1–8.

[15] Samir, A., El-Nashar, D. E., Ashour, A. H., Medhat, M. and El-kameesy, S. U. (2019). Polyvinyl chloride/styrene butadiene rubber polymeric blend filled with bismuth subcarbonate $(BiO)_2CO_3$ as a shield material for gamma rays. *Polymer composites,* 1-9.

[16] Liang, D., Ding, Z., Yan, Q., Hasanagic, Fathi, L., Yang, Z., Li, Wang, J., Luo, H. and Wang, Q. (2023). a primary study on mechanical properties of heat-treated wood via in-situ synthesis of calcium carbonate. *Journal of reneweal materials,* 11 (1): 435-451.

[17] Ervina, J., Mariatti, M., & Hamdan, S. (2016). Effect of Filler Loading on the Tensile Properties of Multi-walled Carbon Nanotube and Graphene Nanopowder filled Epoxy Composites. *Procedia Chemistry, 19, 897–905.* doi: 10.1016/j.proche.2016.03.132.

[18] Ozsoy, I., Demirkol, A., Mimaroglu, A., Unal, H. and Demir, Z. (2015). The influence of micro and nano-filler content on the mechanical properties of epoxy composites. *Journal of mechanical engineering,* 61 (10): 601-609.

[19] Abraham, A., Soloman, P. A., & Rejini, V. O. (2016). Preparation of Chitosan-Polyvinyl Alcohol Blends and Studies on Thermal and Mechanical Properties. *Procedia Technology,* 24, 741–748. doi: 10.1016/j.protcy.2016.05.206.

[20] Ugur, K., Sherif, M. M. and Ozbulut, O. E. (2019). Tensile properties of graphene nanoplatelets/epoxy composites fabricated by various dispersion techniques. *Polymer testing,* 76, 181-191.

[21] Dasan, Y. K., Bhat, A. H., and Faiza, A. (2017). Polymer blend of PLA/PHBV based bionanocomposites reinforced with nanocrystalline cellulose for potential application as packaging materials. *Carbohydrate polymers,* 157, 1323-1332.

[22] Zheng, N., Wu, D., Sun, P., Liu, H., Lou, B. and Li, L. (2019). Mechanical properties and fire resistance of magnesium-cemented popular particleboard. *Materials,* 12 (19): 3161.

[23] Tan, W. C. (2020). Characterisation and Development of New Bio-filler using Mimusops Elengi Seed shells Powder for Polypropylene Composites. *A dissertation submitted to the Faculty of Engineering and Green Technology, University Tunku Abdul Rahman, in partial fulfillment of the requirements for the degree of Master of Engineering Science.*

[24] Tarani, E., Chrysafi, I., Kállay-Menyhárd, A., Pavlidou, E., Kehagias, T., Bikiaris, D. N., Chrissafis, K. (2020). Influence of Graphene Platelet Aspect Ratio on the Mechanical Properties of HDPE Nanocomposites: Microscopic Observation and Micromechanical Modeling. Polymers, 12 (8), 1719.

[25] Rashid, B., Leman, Z., Jawaid, M., Ghazali, M. and Ishak, M. (2016). Physicochemical and thermal properties of lignocellulosic fiber from sugar palm fibers: effect of treatment. *Cellulose,* 23 (5), pp. 2905-2916.

[26] Jia, P., Hu, L., Zhang, M., & Zhou, Y. (2015). TG-FTIR and TG-MS analysis applied to study the flame retardancy of PVC–castor oil-based chlorinated phosphate ester blends. *Journal of Thermal Analysis and Calorimetry,* 124 (3), 1331–1339.

[27] Hajibeygi, M., Maleki, M., & Shabanian, M. (2018). The effects of poly (amide-imide) coating on the thermal, combustion and mechanical properties of polyvinyl chloride ZnO nanocomposites. *Progress in Organic Coatings,* 122, 96–106.

[28] Damilalo, O., Ighalo, J., Adeniyi, A. and Hammed, K. (2020). Morphological and Thermal Properties of Polystyrene Composite Reinforced with Biochar from Plantain Stalk Fibre. *Material International,* 2 (2): 0150-0156.

[29] Kim, M. H., Hwang, C. H., Kang, S. B., Kim, S., Park, S. W., Yun, Y.-S., & Won, S. W. (2015). Removal of hydrolyzed Reactive Black 5 from aqueous solution using a polyethylenimine-polyvinyl chloride composite fiber. *Chemical Engineering Journal, 280, 18–25.*

[30] Mostafa, H., Airouyuawa, J. O., and Maqsood, S. (2022). A novel strategy for producing nano-particles from date seeds and enhancing their phenolic content and antioxidant properties using ultrasound-assisted extraction: A multivariate based optimization study. *Ultrasonic sonochemistry*, 87, 106017.

[31] Abdelghany, A. M., Meikhail, M. S. and Asker, N. (2019). Synthesis and structural-biological correlation of PVC/PVAc polymers. *Journal of materials Research and technology,* 8 (5): 3908-3916.

[32] Praveena, B. A., Santhosh, N., Abdulrajak, B., Srikanth, H. V., Shankar, G., Ramesha, K., Manjunath, N., Karthik, S. N., Rudra, N. M., and Praveen K. S. (2022). Experimental Investigation on Density and Volume Fraction of Void, and Mechanical Characteristics of Areca Nut Leaf Sheath Fiber-Reinforced Polymer Composites. *International Journal of Polymer Science* 1-13.

[33] Han, X., Lu, X., & Vogt, R. D. (2019). An optimized density-based approach for extracting microplastics from soil and sediment samples. *Environmental Pollution,* 113009.

[34] Hanana, F. E. and Rodrigue, D. (2021). Effect of particle size, fiber content, and surface treatment on the mechanical properties of maple-reinforced LLDPE produced by rotational molding. *Polymers and Polymer Composites,* 29 (5): 343–353.

[35] Turku, I., Keskisaari, A., Kärki, T., Puurtinen, A., & Marttila, P. (2017). Characterization of wood plastic composites manufactured from recycled plastic blends. *Composite Structures,* 161, 469–476.